Supplemental Information for

Redox sorting of carbon nanotubes

Hui Gui[1], Jason K. Streit[2], Jeffrey A. Fagan[2], Angela R. Hight Walker[3], Chongwu Zhou[4]* and Ming Zheng[2]*

[1]Department of Chemical Engineering and Materials Science, [4]Department of Electrical Engineering, University of Southern California, Los Angeles, California 90089, USA

[2]Materials Science and Engineering Division, [3]Semiconductor and Dimensional Metrology Division, National Institute of Standards and Technology, 100 Bureau Drive, Gaithersburg, Maryland 20899, USA

***Corresponding Authors: ming.zheng@nist.gov, chongwuz@usc.edu**

Disclaimer: Certain commercial equipment, instruments, or materials are identified in this paper in order to specify the experimental procedure adequately. Such identification is not intended to imply recommendation or endorsement by the National Institute of Standards and Technology, nor is it intended to imply that the materials or equipment identified are necessarily the best available for the purpose. Unless noted otherwise, all reagents were obtained from standard sources.

Materials and Methods

Hanwha (HW) SWCNTs were purchased from Hanwha Chemical. Raymor SWCNTs were purchased from Raymor Nanotech (lot number: RNL 13-020-016). Two sources of HiPco were used in this work, one was purchased from Rice University (batch number: 195.3), and the other from Unidym. Polyethylene glycol (PEG, 6 KDa, Alfa Aesar), dextran (DX, 70 KDa, TCI), sodium deoxycholate (SDC, Sigma-Aldrich), sodium cholate (SC, Sigma-Aldrich), sodium dodecyl sulfate (SDS, Sigma-Aldrich), NaClO (Sigma-Aldrich), dithiothreitol (DTT, Sigma-Aldrich), $NaBH_4$ (Sigma-Aldrich), $KMnO_4$ (Sigma-Aldrich), K_2IrCl_6 (Sigma-Aldrich) and vitamin E ((Sigma-Aldrich) were used as received.

SWCNT dispersion, separation, and purification by centrifugation and by ATP: We follow procedures disclosed in previous publications.[1-3] All the ATP experiments were done at ≈ 20 °C.

Gel column preparation: As received Sephacryl S 100 gel (GE Healthcare) was washed three times with DI water prior to use to remove ethanol from the as received gel slurry. The washed gel was then loaded into a 1 cm-diameter, 3mL, syringe column with a piece of cotton at the bottom to act as a filter for retaining the gel. After settling, the height of the gel column used in the reported results was 2.5 cm. The column was then equilibrated to experimental conditions by passing through a volume of 1% SDS before the SWCNT dispersion was loaded at the top interface for separation.

Optical absorption characterization: A Varian Cary 5000 spectrophotometer was used to measure the UV-visible-near infrared (UV-vis-NIR) absorption of the nanotubes. For samples in which the interesting features were at wavelengths shorter than 1400 nm, we used a quartz microcuvette with 10 mm path length. For samples characterized at wavelengths ≥ 1400 nm, a

cuvette with a 2 mm path length was used. In either instance, blank ATP phases (*i.e.* formed in the absence of SWCNTs at otherwise equivalent compositions) were used to set the reference background, with the corresponding reference phase used as reference when measuring each ATP top or bottom phase sample.

Resonance Raman spectroscopy and RBM assignment: Raman measurements were performed according to previously published procedures.[2] RBM assignments are made according to literature reports.[4,5]

Special notes on oxidants and reductants: Oxidants employed in the study include: NaClO, an inexpensive but effective oxidant; K_2IrCl_6, a strong one-electron oxidant used previously for SWCNT redox chemistry;[6] and $KMnO_4$, a commonly used strong oxidant. For reductants, we have tested dithiothreitol (DTT), which has been used by others to enhance fluorescence quantum yield of semiconducting SWCNTs;[7] $NaBH_4$, a very strong reductant that has been used in conjunction with benzyl viologen to create stable n-doped SWCNTs;[8] and vitamin E, a useful reductant for non-polar solvents.

- $NaBH_4$

  1M $NaBH_4$ in water was freshly prepared just prior to use., as $NaBH_4$ reacts with water and generates H_2 slowly. When calculating the concentration of $NaBH_4$ used in our experiments, we have ignored the reaction and assumed it as 1M.

- NaCLO

  The oxidant NaClO was purchased in liquid form with a specified Cl weight percentage within the range of 10% - 15% by the manufacturer. This corresponds to a NaClO concentration of (3 to 5) M as received. When concentrations of NaCLO are specified in

this contribution the values were calculated assuming a NaClO stock concentration of 5 M.

Experimental details for Figure 1

Table S1. Compositions of the five ATP systems shown in **Figure 1** reporting the volume of each component added. In the shown experiment, each number reports the volume of the component noted in μL.

	20% DX	50% PEG	10% SC	10% SDS	2% SC dispersed HW	Redox chemicals	DI water
Reduced	150	60	40	20	25	100 (1M $NaBH_4$)	115
Semi-reduced	150	60	40	20	25	35 (1M $NaBH_4$)	180
Ambient	150	60	40	20	25	0	190
Semi-oxidized	150	60	40	20	25	5 (50mM NaClO)	185
Oxidized	150	60	40	20	25	2 (0.5M NaClO)	188

For each separation case, we first add all the chemicals into a 1.5 mL Eppendorf tube. This is followed by vortexing the mixture for about 15 s, and centrifugation to settle the two-phase partitioning. The absorption spectra of the "semi-reduced" and "semi-oxidized" separations are shown in **Figure S1**. It is evident that in the "semi-reduced" case, semiconducting SWCNTs are enriched in the bottom phase; whereas in the "semi-oxidized" case, they are in the top phase.

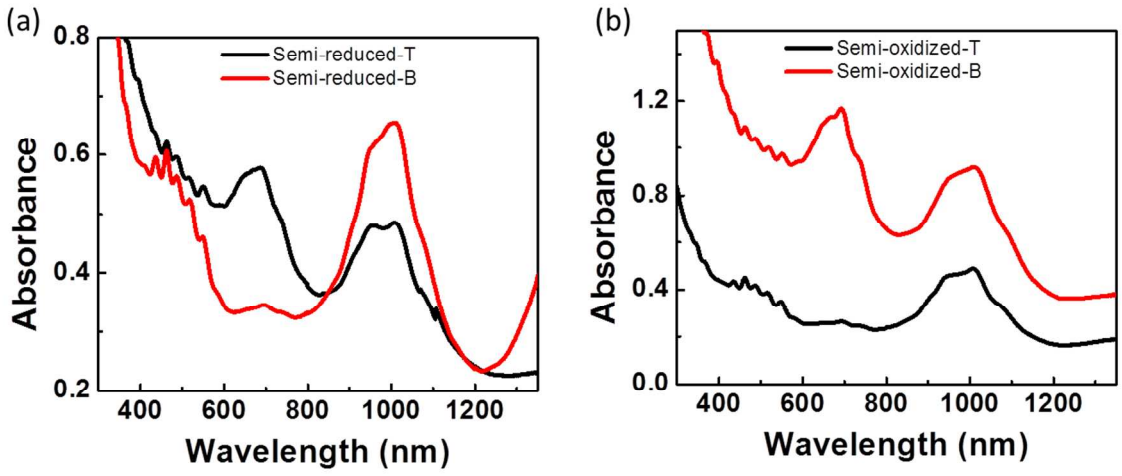

Figure S1. The absorption spectra of (a) "semi-reduced" top (T) and bottom (B) phase, and (b) "semi-oxidized" top (T) and bottom (B) phase.

In this experiment, 40 mM DTT can be used in place of $NaBH_4$ to create the "semi-reduced" regime, but it is not strong enough to achieve the "reduced" regime. The NaClO effect can be reproduced with ≈ 250 mM H_2O_2, or ≈ 20 mM $K_3Fe(CN)_6$, or ≈ 50 μM $KMnO_4$, or ≈ 1 μM K_2IrCl_6.

Experimental details for Figure 2

For successive extractions, the total volume of the constructed two-phase system was increased to 1.5mL to increase the absolute quantity of purified materials obtained. Chemical composition of the ATP system is given in **Table S2**.

Table S2. Composition of the ATP system for NaClO aided successive extraction of HiPco tubes. The volume number unit used in the table is μL.

20% DX	50% PEG	10% SC	10% SDS	2% SC dispersed HiPco	DI water
450	180	75	150	600	45

This composition gives a final concentration of 6% PEG, 6% DX, 0.9% SC, and 1% SDS. The HiPco (Rice) dispersion used in this experiment is first dispersed in 2% SDC. Prior to this experiment, the nanotube dispersion was purified by rate-zonal centrifugation as previously described[2,3] to remove non-nanotube impurities and defective nanotubes such that the optical properties of the dispersion are more prominent; the dispersion was then exchanged into 2% SC using a Millipore stirred ultrafiltration cell.[2,3] The ATP extraction process begins by adding all the chemicals into a 1.5 mL Eppendorf tube. This is followed by vortex-mixing for 15 s, and centrifugation for about 1 min to separate the two phases. Initially, all the SWCNTs are found in the top phase. Because of concern that trace quantities of sodium deoxycholate (SDC) may have been present from the rate-zonal purification, we removed the separated bottom phase (which contains no nanotubes but will contain a roughly volumetric quantity of all surfactants) and replaced it with a fresh blank bottom phase. We then mixed and phase-separated the mixture again (all SWCNTs remaining in the top phase); this process of removing the bottom phase and replacing it with fresh bottom phase (no SDC) was repeated for 3 times to ensure that no trace amounts of SDC remained in the ATP system. At this stage 1mM NaClO was added to push all the SWCNTs to the bottom phase (similar to the oxidizing condition shown in Figure 1). After vortex mixing and centrifugation (in which the PEG acts to partially reduce the applied oxidant concentration), the top phase was found to contain SWCNTs. This top layer was extracted to

yield fraction S1. Then, an equal amount of fresh blank top phase (1mL) as the extracted volume was added, (prepared beforehand to have the composition given in **Table S2**) and the contents mixed. Repetition of the mixing, centrifugation, and top phase extraction steps yields fraction S2. After this, fresh blank top phase (0.5mL) was again added. After mixing and centrifugation, the remaining SWCNTs come to the top (being the M fraction). Another 1 mM of NaClO was then added to push the nanotubes back to the bottom phase, and the same extraction process as noted above was performed to generate fractions M1 to M6. For the metallic tube extraction, the volume of added top phase at each cycle of the process was 0.5 mL. This was chosen to avoid unnecessary dilution of the SWCNT concentration in each fraction.

Experimental details for Figure 3

For the "control" dispersion, PFO-bipy at 1 mg /mL and HiPco material at 0.036 mg/mL were mixed with 1 mL of toluene in a 1.5 mL Eppendorf tube. The mixture was sonicated for 20 min at 8W power output using a 2 mm diameter probe sonicator. The resulting suspension was then centrifuged at 18 ºC and 17,000 g for 5 min. The supernatant is taken as the "control" dispersion.

For the "vitamin E added" dispersion, the same procedure was followed except that 10 mM vitamin E was included in the sonication mixture.

For the "water treated" dispersion, 100 uL of the "control" dispersion was mixed with 10 uL of water and bath sonicated for 5 min. The resulting emulsion was then centrifuged, and the top clear phase taken out to yield the "water treated" dispersion.

Experimental details for Figure S2

For **Figure S2**, a density gradient containing water-filled electric arc nanotubes[9] was prepared and run in a preparative ultracentrifuge (Beckman L80-XP) to demonstrate the change in SWCNT density with the solution redox condition. Eight, three-layer gradients consisting of a 3.7 mL (26 % (volume/volume) iodixanol, 1.125 % SC, 1.125 % SDS) top layer, ≈ 0.7 mL middle layer (30 % iodixanol, 1.125% SC, 1.125 % SDS) containing the dispersed SWCNTs, and a 0.5 mL bottom layer (34 % iodixanol, 1.125 % SC, 1.125 % SDS) were constructed in Beckman optiseal ½" centrifuge tubes (#362185). These solution conditions were chosen to mimic conditions identified previously in our group[9] that led to good metallic/semiconducting separation during DGU.

Prior to constructing the gradients in the centrifuge tube, an amount of either oxidant, 100 X diluted 5 M stock NaClO, or reducing agent, 1 M DTT, was added to both the top and middle layers for each specific centrifuge tube to generate a range of solution redox conditions, including a no additive (ambient) condition. A photograph of one tube showing the constructed density gradients prior to centrifugation and noting the amount of modifier added is shown in **Figure S2a**. The tubes were then ultracentrifuged (VTi 65.2 rotor) at 6810 rad/s (65 kRPM) for 1 h at 20 °C. **Figure S2b** is a photograph of the results; the addition of oxidant dramatically changes the average density of the SWCNTs, whereas the change with addition of the reducing agent is less dramatic. However, close inspection notes that the color at the top of the main SWCNT band changes from blue-gray to bronze with the addition of the reducing agent. The best separation of metallic and semi-conducting tubes was achieved for addition of 2.5 μL/mL (or 0.125 mM) of the oxidant, followed by the ambient conditions. Absorbance spectra of the top and bottom bands for these two samples show clear metal-semiconducting separation

(**Figure S2c**); the spectra are normalized to one at 810 nm to aid comparison. The approximate positions of the extracted bands are shown for each fraction corresponding to the color of the absorbance trace; the spectra of the parent dispersion are shown by the black trace.

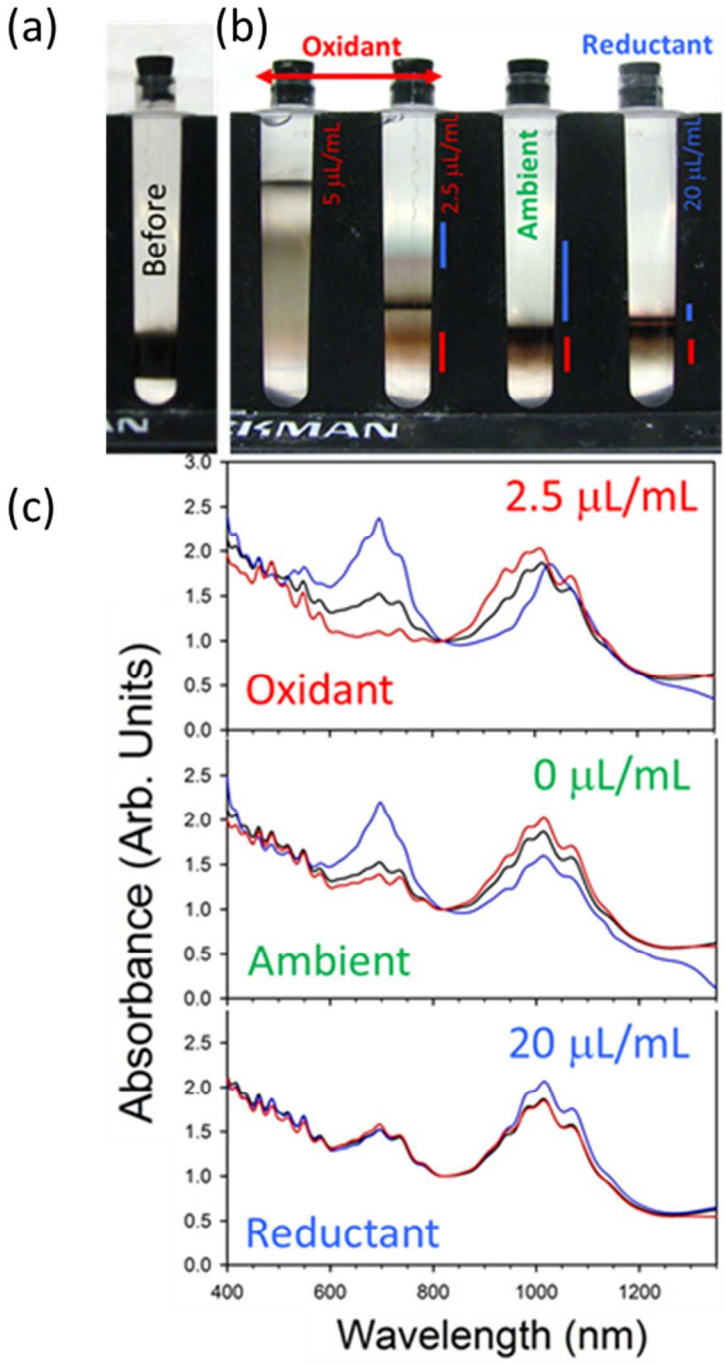

Figure S2 Before (a) and after (b) photographs of a density gradient ultracentrifugation separation with a range of added redox potential altering concentrations. The separation of metallic (light blue) SWCNTs from the semiconducting (bronze) SWCNTs is improved from the ambient condition by addition of the small amount of oxidant NaClO (0.125 mM). Addition of 20 mM reductant DTT reverses the nature of the SWCNTs isolated at the top of the band. Spectra of aliquots collected from three of the tubes are shown in (c); the location of the aliquots is given by the colored bar corresponding to the trace color on the photograph, the pre-separation spectrum is given as the black trace.

Experimental details for Figure S3

For gel chromatographic separation, 0.2 mL HiPco (Unidym) SWCNTs dispersion was loaded onto the prepared gel column. Nanotubes are found to stay in the top of the gel column. A solution of 1% SDS is used to elute nanotubes. The elution is collected at 0.15 mL per fraction.

To examine the redox effect, we treated aliquots of the same HiPco dispersion under three different conditions before loading it onto the gel column: 50 mM DTT added to the HiPco dispersion, nothing added to the HiPco dispersion, and 50 mM NaClO added the HiPco dispersion. The separation outcome of DTT treated HiPco dispersion is shown in **Figure S3a**. When washed by 1% SDS, a red band comes down first, and then the blue band mixed with the red band. The remaining back materials stuck on the column are most likely amorphous carbon impurities, as this dispersion was not extensively prepurified. Absorption spectra of selected fractions are shown in **Figure S3d.** The measurement shows that the early red fraction is metallic enriched (black trace M), whereas the later blue to brown fraction are enriched in

semiconducting SWCNT species. We measured one early and one late S-SWCNT fractions (S1 and S2) and found that the elution order is small-diameter S-SWCNTs first and large-diameter S-SWCNTs second.

The non-treated HiPco dispersion was found to have a different elution pattern as shown in **Figures S3b and S3e**. In this case the early metallic fractions contained a substantial amount of semiconducting SWCNTs as contaminants. For the later semiconductor enriched fractions, larger-diameter tubes came out first followed by small-diameter tubes (opposite to the reducing condition).

Figures S3c and S3f show the elution pattern for the 50mM NaClO treated HiPco dispersion. In this case, two well separated bands are developed. The earlier band is enriched in metallic tubes but has substantial semiconducting tube contamination. The later bands contain mostly semiconducting tubes but displays little diameter separation.

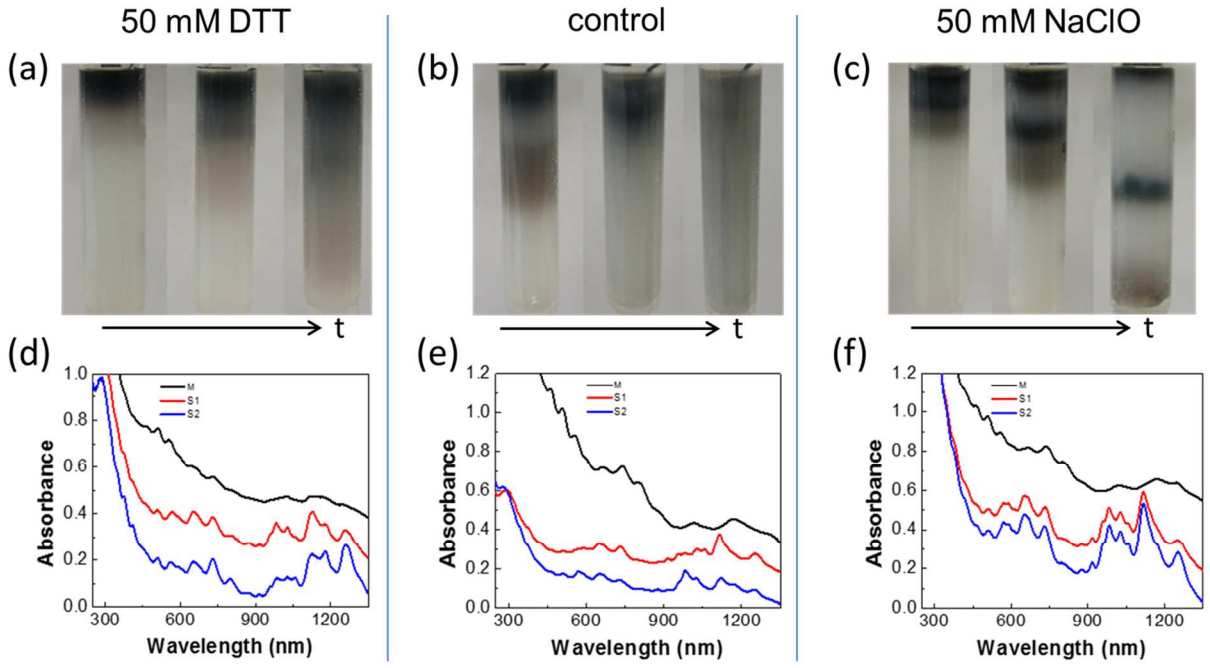

Figure S3 Gel chromatography elution pattern for (a) and (d): DTT–treated HiPco tubes; (b) and (e): non-treated HiPco tubes, and (c) and (f): NaClO-treated HiPco tubes. The three column pictures in each case are taken at the early, middle, and late stage of the elution process.

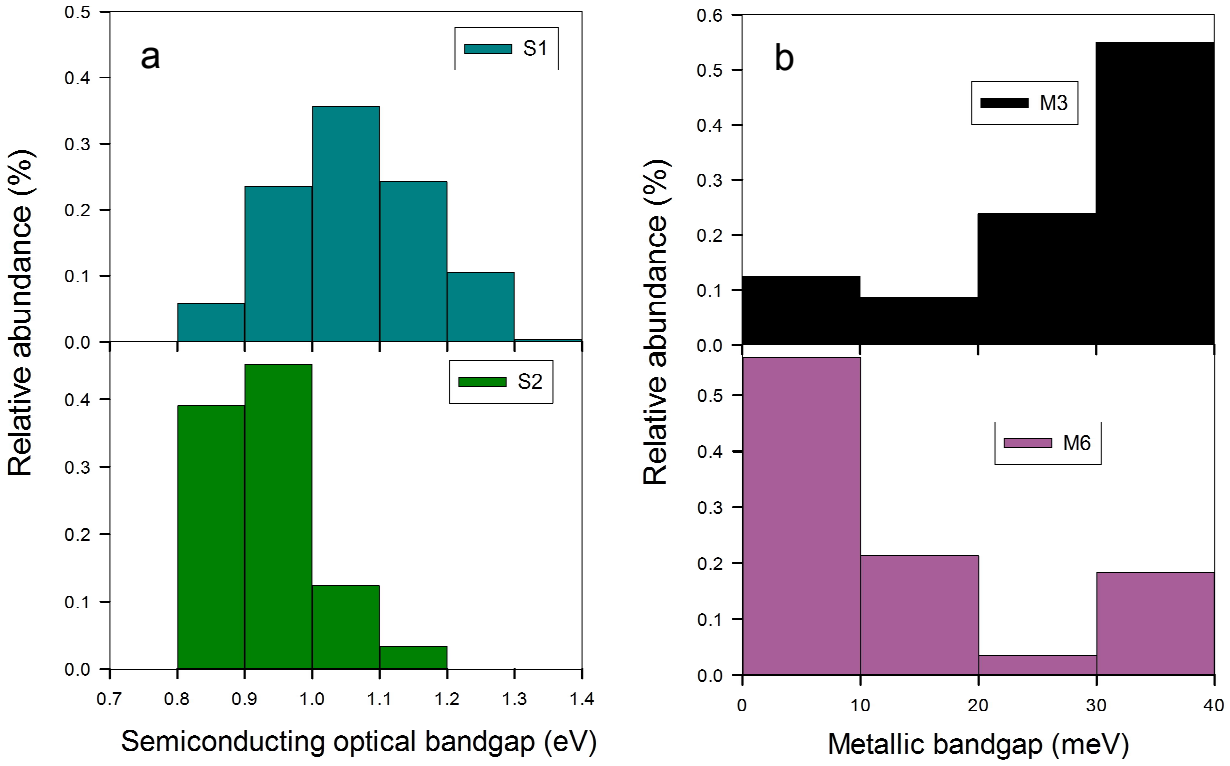

Figure S4 Bandgap distributions of the extracted semiconducting (a) and metallic (b) fractions.

Figure S4 compares bandgap distributions calculated for fractions S1, S2, M3 and M4 shown in Figure 2b and Figure 3a of the main text. Figure S4a shows that smaller diameter (larger bandgap) SWCNTs are first extracted in S1 followed by larger diameter (smaller bandgap) SWCNTs in S2. Figure S4b demonstrates that this oxidative extraction method is additionally able to fractionate metallic nanotubes by their vanishingly small bandgap, with fraction M3 enriched in larger non- zero bandgap semi-metals and fraction M6 enriched in zero-bandgap armchair metals.

For each semiconducting fraction, relative abundances were estimated by analyzing the corresponding absorption spectra (Figure 2b). After subtracting a linear background, Voigt profiles were applied to spectrally simulate the resonant E_{11} absorption peaks of each identified (*n,m*) species. Assuming a similar absorption cross section for each nanotube structure, the relative concentrations were found from the spectrally integrated values obtained from the fitting, each normalized by the sum of all integrated absorbance peaks. The optical bandgap was then determined from the positions of the simulated absorption peaks and the results were binned into a histogram.

Due to the many spectrally overlapping peaks found in the metallic region of the absorption spectrum, Raman measurements (shown in Figure 3b of the main text) were instead analyzed to estimate the relative abundances of metallic fractions M3 and M6. For each fraction, Raman data obtained from each of the three excitation wavelengths were spectrally integrated using Lorentzian profiles to approximate the RBM peaks of the different (*n,m*) structures. To correct for differences in concentration, the integrated RBM values were scaled by the absorbance values found at the excitation wavelength used to acquire the Raman data. Finally, to calculate relative abundances, each scaled RBM peak was normalized by the sum of all scaled RBM peaks in each of the three Raman measurements. For non-armchair metals, small curvature-induced bandgaps were estimated using the analytical expression derived by Kane and Mele[10]. Armchair species have a finite density of electronic states at the Fermi level and thus possess no electronic bandgap. The results were combined and binned into a histogram.

References

(1) Zhang, M.; Khripin, C. Y.; Fagan, J. A.; McPhie, P.; Ito, Y.; Zheng, M. *Analytical Chemistry* **2014**, *86*, 3980.

(2) Fagan, J. A.; Khripin, C. Y.; Silvera Batista, C. A.; Simpson, J. R.; Hároz, E. H.; Hight Walker, A. R.; Zheng, M. *Advanced Materials* **2014**, *26*, 2800.

(3) Khripin, C. Y.; Fagan, J. A.; Zheng, M. *Journal of the American Chemical Society* **2013**, *135*, 6822.

(4) Haroz, E. H.; Duque, J. G.; Tu, X.; Zheng, M.; Hight Walker, A. R.; Hauge, R. H.; Doorn, S. K.; Kono, J. *Nanoscale* **2013**, *5*, 1411.

(5) Haroz, E. H.; Bachilo, S. M.; Weisman, R. B.; Doorn, S. K. *Physical Review B* **2008**, *77*, 125405.

(6) Zheng, M.; Diner, B. A. *J Am Chem Soc.* **2004**, *126*, 15490.

(7) Lee, A. J.; Wang, X.; Carlson, L. J.; Smyder, J. A.; Loesch, B.; Tu, X.; Zheng, M.; Krauss, T. D. *Nano Letters* **2011**, *11*, 1636.

(8) Kim, S. M.; Jang, J. H.; Kim, K. K.; Park, H. K.; Bae, J. J.; Yu, W. J.; Lee, I. H.; Kim, G.; Loc, D. D.; Kim, U. J.; Lee, E.-H.; Shin, H.-J.; Choi, J.-Y.; Lee, Y. H. *Journal of the American Chemical Society* **2008**, *131*, 327.

(9) Fagan, J. A.; Huh, J. Y.; Simpson, J. R.; Blackburn, J. L.; Holt, J. M.; Larsen, B. A.; Walker, A. R. *Acs Nano* **2011**, *5*, 3943.

(10) Kane, C. L.; Mele, E. J. *Physical Review Letters* **1997**, *78*, 1932.